Chemical Bonding to N, P, and As in Ylides and Their Boron Analogues

Angel Sánchez-González,[†] Henar Martínez-García,[‡] Santiago Melchor,[†] and Jose A. Dobado*[,†]

Grupo de Modelización y Diseño Molecular, Instituto de Biotecnología, Facultad de Ciencias, Universidad de Granada, E-18071 Granada, Spain, and Departamento de Química Orgánica, ETSII, Universidad de Valladolid, E-47071 Valladolid, Spain

Received: June 7, 2004; In Final Form: August 6, 2004

Ab initio (MP2/6-311+G*) and density functional theory (B3LYP/6-311+G*) calculations have been performed to determine the bonding nature of N, P, and As (pnicogens) with B or C in ylides and their boron analogues. The compounds studied refer to the formulas $R_3XCR'_2$ and R_3XBR' (X = N, P, As; R = H, F; R′ = H, SiH_3). The computed electron density has been analyzed by means of the atoms in molecules (AIM) theory and the electron localization function (ELF) method. In addition, the rotational barriers were calculated for X−C and X−B bonds at the CASMP2/6-311+G* level to elucidate the multiple bonding character for these bonds. The geometric and electronic results indicated that the N ylides differ remarkably from the remaining pnicogen (P, As) ylides, with the former yielding clear single bonds while the latter showed stronger multiple bonds. Moreover, the fluorine substituents strengthened the X−C and X−B bonds, reducing the bond distance, increasing the electron density, and augmenting the planarity at the C and B atoms. However, the SiH_3 groups affected only the planarity at the C atoms for the organic ylides. This indicates how the electronegativity of the different substituents influence the central X−C and X−B bonds: if the substituent pulls charge from the bond in the direction toward the pnicogen, the bond is reinforced and it is more likely to present double-bond characteristics. This is not accomplished by substituents pushing charge in the aforementioned direction. Differences between the organic ylides and their boron derivatives have been found. Boron analogues presented remarkable asymmetric X−B bonds, with a rotation barrier of ca. 30 kcal/mol, caused by a strong repulsion between the lone pairs of the XH_3 unit and that of boron.

Introduction

Ylides are usually defined as organic molecules that have a contributing Lewis structure with opposite charges on adjacent atoms, each of which has an octet of electrons. Within ylides, the ammonium and phosphonium derivatives have been demonstrated to be extremely useful[1] in organic synthesis as intermediates in the preparation of highly functionalized compounds and as synthons for constructing C═C double bonds. Since the discovery of ylides in 1928 by Stevens,[2] their use and interest have grown rapidly, particularly in recent decades, and now these molecules are considered powerful tools in the synthesis of olefins[3,4] and small rings.[5] Although ylides are mainly organic compounds, the concept can be extended also to a broader set of molecules, including inorganic structures with a zwitterionic character, where carbon is replaced by an heteroatom and thus may not have eight electrons in the external valence shell.

In the above-mentioned simplified scheme, the pnicogen−carbon (X−C) bond is considered to be a conventional single σ-bond, although the interaction between these charged atoms is strengthened due to electrostatic contributions.[6] Within this framework, the carbon atom shows a lone pair and two substituents, while the pnicogen accepts three substituents.

A similar behavior is expected for all the pnicogen ylides, where electronegativity is manifested merely in the polarization of the central bond. However, there are significant geometric differences between N and the remaining pnicogen (P and As) ylides that need further investigation.

Although bonding in ammonium ylides has been clearly determined as a single one,[7] in recent years, the controversy for phosphonium ylides still continues.[8] Although these compounds have been extensively studied, a clear characterization for the central P−C bond remains elusive. On the other hand, there is a clear agreement on its covalency, with a strong polar character, its bond length being determined mainly by electrostatic interactions.[6] Most authors assign it a single nature, based on structural, energetic, and/or electronic studies. The first geometric and conformational studies[9] describe a nonplanar structure for the carbon moiety, supporting a single P−C bond. Moreover, the first rotational-barrier studies on these compounds yielded very low (<1 kcal/mol) values, also supporting this single-bond character.[10−12] It is noteworthy that, although these authors clearly supported a single P−C bond, they also kept open the possibility of a double P═C one. In addition, Nyulászi reported similarities between the P−C bond in ylides and the standard P═C bond, explaining the bonding nature as a pure ylene form,[11,12] while trying to discard completely the ylide form. On the other hand, we recently calculated the NMR chemical shifts in some of these compounds,[6] finding values very similar to those of standard single bonds.

The typical bonding scheme for these compounds is explained by contributions to the ylide and ylene forms depicted in Scheme 1, which accounts for the relative multiple character of some ylides. Nevertheless, the ylene form requires a dsp^3 hybridization to allow a multiple bond for P and As atoms, but not for N. This possibility was discarded, and there is general agreement

* Corresponding author. E-mail: dobado@ugr.es.
[†] Universidad de Granada.
[‡] Universidad deValladolid.

10.1021/jp047555r CCC: $27.50
Published on Web 09/17/2004

SCHEME 1: Ylide and Ylene Forms (X = P and As)

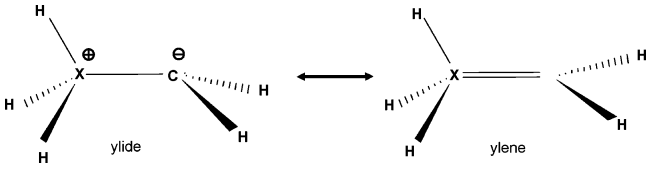

SCHEME 2: Schematic Geometries for Pnicogen−Boron 1−3(a−d) and Pnicogen−Carbon 4−6(a−d) Compounds of the Ylide Series Studied in This Work

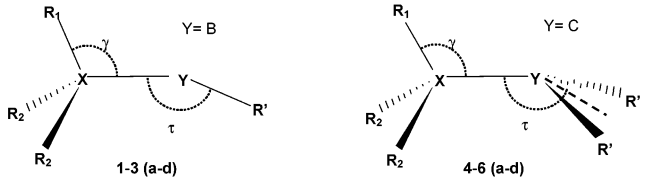

	X	R=R'=H	R=F, R'=H	R=H, R'=SiH_3	R=F, R'=SiH_3
	N	**1a**	**1b**	**1c**	**1d**
Y=B	P	**2a**	**2b**	**2c**	**2d**
	As	**3a**	**3b**	**3c**	**3d**
	N	**4a**	**4b**	**4c**	**4d**
Y=C	P	**5a**	**5b**	**5c**	**5d**
	As	**6a**	**6b**	**6c**	**6d**

that the computational use of a d shell is necessary only as polarization functions, not participating in the bonding.[13−16] Different molecular orbital (MO) calculations support the possibility of a double bond,[8] describing a HOMO that consists of a carbon p_x orbital extended clearly to the phosphorus. Another fact that reveals a strong interaction is the short P−C bond distance (ca. 1.670 Å),[6] not much longer than a standard double P═C bond, and a bond strength similar to that in the $HP{=}CH_2$ compound.

There are also alternative descriptions defining fractional bond orders (about 1.3) between single and double values.[17] An example of the difficulty in assigning a specific P−C bond order has recently been reported, where different interpretations arise from the sharing indices used by Mitrasinovic. Intergroup and interbasin sharing indices yield double- and single-bond interpretations, respectively.[18−20]

All the above highlights the need to clarify and analyze the main differences in the pnicogen ylide series, in order to understand their respective bonding to carbon. In the present work, we focus on ylides with a negative charge on the carbon atom, and we extend this study to their boron analogues. These two first-row elements show different abilities in filling their valence shell and therefore will be used to test the dependence of the bonding characteristics on the population of the valence shells. We have performed ab initio and density functional theory (DFT) calculations for a series of compounds (see Scheme 2), with different substituents (R, R′ = H, F, SiH_3) that are expected to change the central X−C and X−B bond properties. The electron density has been analyzed by means of the atoms in molecules theory (AIM) and the electron localization function (ELF) in order to locate the electron pairing regions, shedding light on the chemistry involving these compounds. Additionally, rotational barriers have also been computed to explore the differences in the bonding nature caused by the substituents.

Methodology

Ab initio and DFT calculations, at the Møller−Plesset[21] second-order-corrected (MP2) and B3LYP[22,23] theoretical levels, respectively, have been performed with the 6-311+G* basis set for the pnicogen−carbon **1**−**3**(**a**−**d**), and pnicogen−boron **4**−**6**(**a**−**d**) ylides studied, using the Gaussian98[24] program. All the structures were fully optimized using the above-mentioned MP2/6-311+G*//MP2/6-311+G* and B3LYP/6-311+G*//B3LYP/6-311+G* theoretical levels, with all the structures yielding true minima and showing no imaginary frequencies. Due to the different characteristics and advantages of B3LYP and MP2 methodologies, we decided to compute each physical magnitude with the best available method. Although both methods include the electronic correlation, the MP2 provides more accurate geometries and precise energies. Nevertheless, the description of the electronic structure, and particularly the electronic density, is best given by density functional methods such B3LYP, due to the explicit consideration of the electronic density as the magnitude that is optimized variationally. This is why B3LYP-obtained wave functions have been employed in the following electronic structure analyses.

The atoms in molecules (AIM) theory explores the topology of electron density and describes accurately the chemical concepts of atom, bond, and structure.[25,26] Another complementary electron-density-based topological analysis which provides useful information on the bond structure is the electron localization function (ELF), as defined by Becke and Edgecombe.[27] The AIM and ELF analyses have been carried out from the computed B3LYP/6-311+G*//B3LYP/6-311+G* electron density, with the AIMPAC[28] and ToPMoD[29] software packages. The ELF plots consist of the ELF isosurfaces at a fixed value of 0.7, and were obtained with the SciAn[30] scientific visualization program. The color convention represents core basins in magenta, and the remaining valence basins are classified depending on their synaptic order:[31] red for monosynaptic, green for disynaptic, and cyan for disynaptic hydrogenated basins.

Rotational barriers were calculated using the multiconfigurational CASMP2/6-311+G*//MP2/6-311+G* method, with an active space of two electrons and two MOs. Complete active space calculations were performed and compared in order to determine more precisely the barrier heights, through a correct determination of the electronic state in the geometries near the maxima.

The rotational barriers were calculated for compounds **1**, **2**, **4**, and **5**(**a**,**b**), starting from the minimum structures optimized at MP2/6-311+G* level, and modifying only the $R_1{-}X{-}Y{-}Z$ dihedral angle (where R_1 lies on the symmetry plane and Z is the centroid of all R′ substituents; see Scheme 2). The remaining geometric parameters were kept frozen during the potential energy scan in order to preserve the electronic environment around the pnicogen, because the rearrangement of the substituents leads to the same conformation every 120°, masking the presence of a possible double bond.

Results and Discussion

I. Geometry and Energetic Stability. We performed a series of theoretical calculations on the molecules described in Scheme 2, corresponding to the R_3XBR' and $R_3XCR'_2$ formulas (where X = N, P, and As).[32] Table 1 lists the geometric parameters calculated at the MP2/6-311+G*//MP2/6-311+G* level for all **1**−**6**(**a**−**d**) structures, while the AIM electronic data calculated at the B3LYP/6-311+G*//B3LYP/6-311+G* level are tabulated in Table 2. The main geometric trend consisted of the shortening

TABLE 1: Geometric Parameters for Compounds 1−6(a−d): X−Y, R_1−X, R_2−X, and Y−R′ Bond Distances, Angles τ and γ, and Bond Dissociation Energies E_{BDE}, Calculated at the MP2/6-311+G*//MP2/6-311+G* Level

		D^a (Å)	D_{R_1X} (Å)	D_{R_2X} (Å)	$D_{YR'}$ (Å)	τ^a (deg)	γ^a (deg)	E_{BDE} (kcal/mol)
1a	H_3N-BH	1.691	1.012	1.022	1.230	97.0	116.6	16.5
2a	H_3P-BH	1.987	1.442	1.402	1.214	110.6	142.9	13.1
3a	H_3As-BH	2.163	1.554	1.510	1.221	106.4	147.0	7.4
4a	H_3N-CH_2	1.551	1.027	1.015	1.098	113.5	120.2	18.2
5a	H_3P-CH_2	1.678	1.438	1.403	1.085	148.7	129.4	46.7
6a	H_3As-CH_2	1.817	1.555	1.507	1.090	132.9	135.2	30.6
1b	F_3N-BH	1.455	1.785	1.357	1.183	124.0	127.2	22.3
2b	F_3P-BH	1.904	1.610	1.572	1.198	119.2	146.6	11.2
3b	F_3As-BH	2.145	1.773	1.731	1.211	112.8	158.0	2.8
4b	F_3N-CH_2	1.313	1.722	1.359	1.079	157.7	121.6	52.5
5b	F_3P-CH_2	1.613	1.586	1.583	1.081	164.2	126.5	59.8
6b	F_3As-CH_2	1.756	1.747	1.712	1.087	139.2	135.2	31.0
1c	$H_3N-BSiH_3$	1.650	1.028	1.020	2.060	103.2	120.3	122.6
2c	$H_3P-BSiH_3$	1.913	1.441	1.403	2.018	112.6	136.6	189.2
3c	$H_3As-BSiH_3$	2.067	1.551	1.508	2.043	107.2	139.9	346.0
4c	$H_3N-C(SiH_3)_2$	1.499	1.023	1.024	1.809	178.6	115.7	202.8
5c	$H_3P-C(SiH_3)_2$	1.676	1.422	1.408	1.833	176.8	122.8	300.6
6c	$H_3As-C(SiH_3)_2$	1.797	1.531	1.509	1.833	173.4	122.8	447.1
1d	$F_3N-BSiH_3$	1.441	1.776	1.356	1.998	126.4	125.2	173.7
2d	$F_3P-BSiH_3$	1.863	1.607	1.570	1.996	123.0	140.2	225.0
3d	$F_3As-BSiH_3$	2.117	1.776	1.729	2.046	117.3	153.6	374.2
4d	$F_3N-C(SiH_3)_2$	1.304	1.711	1.384	1.887	164.6	119.7	267.8
5d	$F_3P-C(SiH_3)_2$	1.607	1.578	1.565	1.857	176.7	120.5	347.9
6d	$F_3As-C(SiH_3)_2$	1.729	1.734	1.717	1.865	172.1	124.7	478.5

[a] See Scheme 2 for definition.

TABLE 2: Electronic Properties for X−Y Bonds in 1−6(a−d): Electron Density at the Bond Critical Point $\rho(r_c)$, Its Laplacian $\nabla^2\rho(r_c)$, Ellipticity ϵ, and Electronic Energy Density E_d, Delocalization Index between X and Y Basins δ(X,Y), and Total Charges Integrated over X and Y Basins q_X and q_Y, Computed at the B3LYP/6-311+G*//B3LYP6-311+G* Level

		$\rho(r_c)$ (e a_0^{-3})	$\nabla^2\rho(r_c)$ (e a_0^{-5})	ϵ	$E_d(r_c)$ (hartree a_0^{-3})	δ(X,Y)	q_X (e)	q_Y (e)
1a	H_3N-BH	0.100	0.224	4.49	−0.065	0.60	−1.24	0.64
2a	H_3P-BH	0.109	−0.162	0.29	−0.065	0.92	1.16	0.55
3a	H_3As-BH	0.082	−0.062	0.22	−0.035	0.82	0.68	0.51
4a	H_3N-CH_2	0.173	−0.160	0.26	−0.171	0.92	−0.94	−0.20
5a	H_3P-CH_2	0.115	−0.007	0.44	−0.198	1.20	2.31	−1.16
6a	H_3As-CH_2	0.097	−0.116	0.23	−0.106	1.30	1.16	−0.67
1b	F_3N-BH	0.218	0.627	0.80	−0.207	0.90	−0.09	1.47
2b	F_3P-BH	0.129	−0.226	0.29	−0.085	1.04	1.99	0.72
3b	F_3As-BH	0.081	−0.044	0.11	−0.032	0.80	1.40	0.68
4b	F_3N-CH_2	0.336	0.137	0.37	−0.508	1.38	0.17	0.38
5b	F_3P-CH_2	0.217	0.142	0.72	−0.233	1.16	3.21	−1.26
6b	F_3As-CH_2	0.172	−0.125	0.31	−0.123	1.36	2.12	−0.57
1c	$H_3N-BSiH_3$	0.109	0.268	2.58	−0.072	0.74	−1.27	−0.32
2c	$H_3P-BSiH_3$	0.124	−0.223	0.50	−0.089	1.08	1.15	−0.50
3c	$H_3As-BSiH_3$	0.097	−0.101	0.36	−0.049	1.02	0.67	−0.57
4c	$H_3N-C(SiH_3)_2$	0.201	−0.119	0.43	−0.234	1.04	−1.01	−1.53
5c	$H_3P-C(SiH_3)_2$	0.192	0.000	0.26	−0.195	1.16	2.31	−2.42
6c	$H_3As-C(SiH_3)_2$	0.166	−0.111	0.17	−0.114	1.34	1.21	−2.00
1d	$F_3N-BSiH_3$	0.221	0.672	0.73	−0.209	0.94	−0.13	0.46
2d	$F_3P-BSiH_3$	0.145	−0.298	0.48	−0.117	1.20	1.85	−0.29
3d	$F_3As-BSiH_3$	0.098	−0.076	0.19	−0.044	1.00	1.71	−0.45
4d	$F_3N-C(SiH_3)_2$	0.333	0.328	0.11	−0.498	1.50	0.11	−0.63
5d	$F_3P-C(SiH_3)_2$	0.216	0.147	0.41	−0.230	1.16	3.23	−2.45
6d	$F_3As-C(SiH_3)_2$	0.182	−0.123	0.28	−0.137	1.50	2.19	−1.82

of the central X−Y distance after substituting the hydrogen with F and SiH_3 groups for all compounds **1**−**6**, this effect being much higher in the case of fluorination. For compounds with both substitutions, **1d**−**6d**, the X−Y distance shortened to the minimum values, but the differences between **b** and **d** series were very low, confirming that F substitution was the main responsible for this effect. This shortening differed for **1**−**6**. The bond distance was drastically decreased in ammonium ylides **1b** and **4b**, by 0.236 and 0.238 Å, respectively, while the other variations remained below 0.08 Å. Similar effects were observed in the τ-angle, which measures the degree of planarity at the Y atom. The substitution in both X and Y positions increased the planarity on Y, and again the effects were much more noticeable in the nitrogen compounds, with τ augmenting ca. 27° from **1a** to **1b**, and ca. 44° from **4a** to **4b**. Similarly, the effects of the SiH_3 groups were less pronounced, with the notable exception of the carbon derivatives, where the SiH_3 steric repulsion forced the τ-angle to be close to 180°. All these geometric data are compatible with an increase in the bond multiplicity due to the fluorination next to N, P, and As atoms, being much more noticeable for N compounds, and are accompanied by a reduction in the CH_2 pyramidalization (or in the XBH angle).

Under some circumstances, the XR_3 group presented a different orientation, depending on the substituents attached, and therefore the γ-angle, which measures this orientation, also merits attention. As a general trend, the heading angle γ increased progressively with the size of the X atom; 120−135° is the usual range for carbon compounds and 120−150°, significantly wider, is the range for boron compounds. Only for boron compounds **1b**−**3b** was this angle affected by the fluorine substituents, augmenting γ an average of ca. 10°. For the SiH_3 derivatives **1c**−**6c**, γ is reduced, but not more than 10° for both boron and carbon compounds. This displacement

in the γ values cannot be associated with any repulsion or attraction between substituents, because of their wide separation. This effect is much more noticeable for compounds with second-row and beyond atoms. This effect seems to be produced by a larger electron concentration zone close to the valence shells for P and As, which repels the substituents attached to X. This is shown below in the analysis of the electronic structure.

We compared also the bonding dissociation energies (BDE) for the studied compounds, calculated as the energy difference relative to the fragments R_3X and CR'_2 (or BR'), and corresponding to the heterolytic breakdown of the bond. Homolytic dissociation energies were also computed, but were more energetically unfavorable than the heterolytic ones. The BDEs listed in Table 1 support the effect described above: the strength of N−Y bonds is enlarged, especially for organic ylides, where the BDE rises from 18.2 to 52.5 kcal/mol. On the contrary, the effect of fluorination in the P−Y bonds is less pronounced: before and after fluorination, the strength of the P−C bond in **5a** and **5b** is near 50 kcal/mol, which indicates that **5a** already presented a typically double bond strength that can be only moderately increased with the fluor substituents. This behavior contrasts with that of As compounds, whose bond strength is barely affected by fluorination.

II. AIM Analysis. The main characteristics of the central X−Y bond were analyzed using the AIM theory, through evaluation of the properties of the corresponding bond critical point (BCP) shown in Table 2. The charge density of a BCP usually marks the bond strength, as it measures the population in areas between two bonded atoms where the density is thinnest. To some extent, it also measures the degree of multiplicity, although this analysis must be performed carefully, because the density may be influenced by other phenomena. For the unsubstituted compounds **1a**−**6a**, the electron density usually falls within the range of 0.08−0.12 e a_0^{-3} (except in an abnormally high value for **4a**). If we compare these values with those corresponding to the fluorinated compounds (series **b** and **d**), the density generally is augmented, but to a different degree depending on the pnicogen involved. The density in ammonium ylides almost doubled, while for the rest the increase was less pronounced. Generally, the density in boron compounds with P and As remained almost the same after F substitution, while conventional phosphonium and arsenium ylides still underwent strong modifications induced by the fluorine. On the contrary, the SiH_3 affected only the organic ylides, noticeably increasing the density, because the aforementioned repulsion between both SiH_3 groups forced sp^2 hybridization to the carbon atom and also possibly increased the double-bond character. As this repulsion was possible only for tricoordinated Y atoms, the effects of the SiH_3 groups in boron compounds were negligible.

The same trends were also found for the $E_d(r)$ values. All the $E_d(r)$ data were negative, indicating more stabilized bonds, especially for organic ylides, presenting higher absolute values. The F substituents noticeably increased bond stability, while the SiH_3 groups induced a moderate stabilization, with the ammonium ylides yielding the maximum values.

On the other hand, the Laplacian values calculated at the BCP showed dissimilar results, even for compounds with the same substituents. This result is related to the different electronegativities between N and the remaining P and As atoms. For example, the Laplacian plots for the N and P compounds (see Supporting Information, Figure S1) showed changes in the concentration and depletion charge zones that were less significant than the displacement of the interatomic surface. Consequently, the charges on the X basins were generally much more negative for the N atom. Therefore, the BCP contained in the interbasin surface can be located in the charge-depletion or charge-concentration zones, yielding to positive and negative Laplacian values, respectively. Accordingly, Table 2 presents high positive Laplacian values for most N compounds (except for the **4a** and **4c** ylides). Again, the effects of fluorine were noticeable, as opposed to the SiH_3 ones. Generally, the values increased with the F substituents. Meanwhile, the boron compounds with As and P remained unaffected. Moreover, the steric effects between SiH_3 groups were not reflected in these values, indicating that the repulsion affected only the electronic distribution in the perpendicular direction of the X−Y bond.

After the discussion of the electronic structure changes with the substituents, it is appropriate to compare the ellipticity.[33] The most striking values corresponded to **1a** and **1c**, with unusually high values. The As compounds showed the lowest values, the remaining ones normally being greater than 0.30. For comparison, a conventional C=P double bond shows an ellipticity of 0.39 and and a C−P single bond shows 0.09.[6] The high ϵ-values in **1a** and **1c** can be attributed to a low variation of the electron density in one of the two directions perpendicular to the bond. This indicates a certain predisposition of the BCP to be divided in two, or at least to become a (2,0) critical point instead of a (3,−1). This reflects the relative instability of the electronic structure around these BCPs.

Another parameter usually involved in the bond multiplicity determination is the delocalization index δ(X,Y), which measures the number of electron pairs shared between two neighboring basins. Although it is immediately related to the bond order, there is agreement for δ(X,Y) to usually be lower than the corresponding bond order,[6,34,35] and indeed, the linear relationship between bond order and delocalization index is not proven. In Table 2, we report these indices, some of them calculated previously elsewhere. We may note that most values remained <1 for the unsubstituted **1a**−**6a** molecules. In comparison, with the F-substituted **1b**−**6b**, the changes were clear, but there was also a dependence on the participating pnicogen. The most remarkable changes corresponded to the ammonium ylides **1** and **4**, augmenting the delocalization indices in ca. 50%. The P and As ylides also showed a general increase, but invariably $<10\%$. This was also noted comparing the **c** and **d** series. The delocalization indices δ(X,Y) for single, double, and triple bonds for various molecules are reported in the literature.[6,34,35] For instance, in C−C bonds, these indices take values of 0.95, 1.89, and 2.85 for single, double, and triple bonds,[35] respectively, in a 1:0.95 ratio, while in C−N bonds the values for a single bond and a double bond are 1.04 and 1.79, respectively.[6] Therefore, although the values for **5a** and **5b** remained between those of a P−C single and those of a double bond[6] (0.92 and 1.70, respectively), the increase with respect to 0.92 was notable, similar to the proportional increase between **4a** and **4b**, which has been shown as an abrupt differentiation between single and double bonds, respectively.

From all the above, we can draw some preliminary conclusions that reveal the main electronic characteristics of the bond in those systems. Both SiH_3 and F substitutions at Y and X positions, respectively, induced a push−pull electron displacement throughout the whole molecule from the right to the left (following the orientation in Scheme 2), as can be appreciated in the AIM charges integrated on the X and Y basins (see Table 2). This electron displacement is manifested in the decrease (pull effect) of ca. 1 e for the X basins of the compounds **1b**−**6b**, and in the increase (push effect) of the same magnitude for the Y basins (**1c**−**6c**). In **1d**−**6d**, both effects (push−pull) were

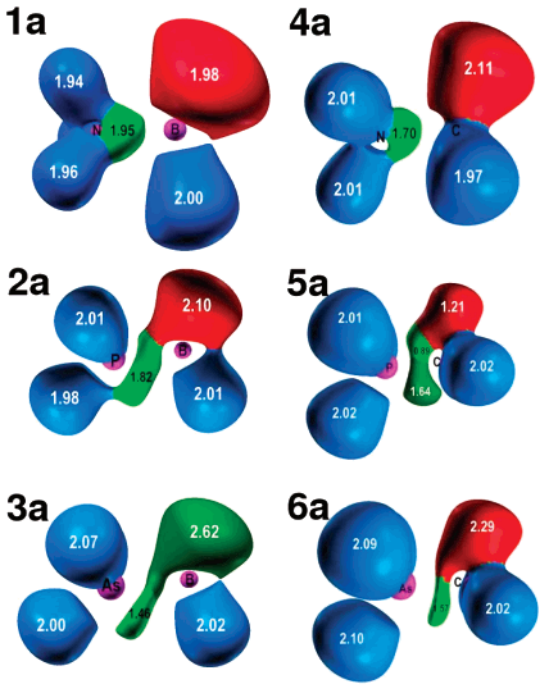

Figure 1. ELF representation at 0.7 for **1a**−**6a**, at the B3LYP/6-311+G*//B3LYP/6-311+G* level.

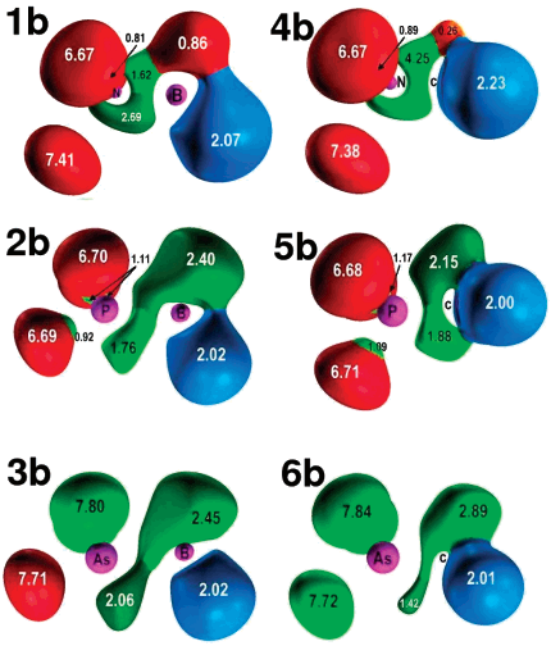

Figure 2. ELF representation at 0.7 for **1b**−**6b**, at the B3LYP/6-311+G*//B3LYP/6-311+G* level.

present, yielding an overall electron displacement throughout the whole molecule. This is associated with two main geometric changes, the shortening of the bond length and the τ-angle, together with electronic differences, and also the increase of the electron density and delocalization indices between X and Y. All these changes are qualitative for nitrogen species **1** and **4**, yielding values compatible with the presence of a double bond for fluorinated compounds. These modifications were slight for the arsenium ylides, producing a very low bond strengthening, while the phosphonium ylides **2** and **5** behaved differently, the latter presenting, overall, more changes than the boron derivative **2**. Moreover, the differences between **5a** and **5b** were clear in the electron density, ellipticity, and τ-angle, with minimal changes for **2**. It is worth mentioning that not all these substantial changes were reflected in the delocalization indices, yielding values of 1.20 and 1.16 for **5a** and **5b**, respectively. This indicates that the delocalization index should not be the only parameter considered in the determination of bond multiplicity.

III. ELF Analysis. After the magnitude of the changes induced by these substitutions was estimated, the electronic structure was analyzed in detail through the representation of the ELF. Figures 1 and 2 show the ELF isosurfaces for **1a**−**6a** and **1b**−**6b**, respectively. Representations of the remaining molecules are included as Supporting Information (Figures S2 and S3). Differences between the ammonium and the remaining phosphonium and arsenium ylides, for unsubstituted compounds **1a**−**6a**, became clear and straightforward in these representations. The ammonium ylides **1a** and **4a** presented only one valence basin (depicted in light green) for the X−Y bonds, located close to the N atom, and showing almost cylindrical symmetry. On the other hand, the remaining compounds presented an elongated shape for this basin, located within the molecular symmetry plane and almost perpendicular to the bond, and in some cases, divided into two or more basins. These results indicated a different bonding scheme for the ammonium and the remaining P and As ylides. The N−B and N−C bonds in **1a** and **4a**, respectively, clearly resembled a dative bond, highly polarized toward the nitrogen, while the remaining molecules presented bonds clearly interacting with the lone pair from the methylene (borylene) moieties, which in some cases appeared as double.

The aspects related to the bond multiplicity have to be discussed carefully, because the limits are not always clear, especially in ylides. In most of the P and As ylides, the X−Y basins were located perpendicularly to the bond and extended toward a monosynaptic basin at the carbon/boron position (depicted in red as monosynaptic) with a varied population. Within the unsubstituted molecules, the most defined bond scheme corresponded to **5a**, where the bond valence basin acquired a standard double-bond shape, and the monosynaptic basin had a very low population of 1.12 e. In the other cases, for **2a**, **3a**, and **6a**, there were only two basins between X and Y atoms, the population of the upper monosynaptic basin being ca. 2 e, with a standard lone-pair configuration at the B and C atoms. It is noteworthy that the frontiers between the fused basins in **2a**, **3a**, and **6a** were numerically undefined and difficult to determine. For example, in **3a** the frontier lies below the As−B bond line, while in **2a** the separation is slightly over the P−B bond (see Figure 1), indicating an almost constant ELF region between the attractors of both basins.

The effects of the F substitution next to X are clearly visible in Figure 2. As discussed above in the AIM analysis, the changes for the nitrogen compounds were the most relevant. The formerly single N−Y basins (**1a**, **4a**) are now split in two (**1b** and **4b**), but the overall population of the new basins was 4.25, larger than twice the former population, and corresponding to two electron pairs. This is because the previous lone-pair basin, at B and C atoms, has been destroyed (almost totally in **4b**), favoring the X−Y central bond and resulting in a clear double-bond character. Moreover, the hybridization changed at carbon (totally) and at boron (partially). This sharp change induced all the geometric and electronic modifications discussed above.

In Figure 2, the N−C valence basin of **4b** appeared as a single one, contrary to **1b**, this being caused by a region of ELF values very close to 1, distributed perpendicularly to the bond. This illustrates again the numerical difficulties in the precise determination of the different attractors and basins in the ELF.

Additionally, the N atom is bonded with single bonds to the two upper F atoms, but the bond with the lower one, located in the symmetry plane, proved to have an ionic character. This was also corroborated by an electron population of 1 e higher and a very long F−N bond distance. All this leads us to consider **1b** and **4b** as complexes formed by F^- and the $F_2NCH_2^+$ and F_2NBH^+ cations, respectively.

The ELF diagrams for the remaining molecules (**2b**, **3b**, **5b**, and **6b**) were in agreement with the above-mentioned trends: the X−Y bond in As ylides showed slight modifications, while the P ylides underwent substantial differences, especially from **5a** to **5b**. In this case, the lone-pair basin at the C atom disappeared completely, although a slight asymmetry between the upper lobe and lower lobe from the double bond still appeared. This was not the case of the boron derivatives **2b** and **3b**, where the shape remained unchanged and only their population and volume increased.

The presence of SiH_3 groups does not generally induce substantial changes in the central X−Y bond, except for the steric repulsion in the organic ylides. For example, the ELF basin for the N−Y bond remained almost unchanged, in contrast to the effect caused by the fluorine. The boron derivatives presented no differences upon SiH_3 substitution, while for organic ylides the lone-pair basin was destroyed, without reinforcing the central X−C bond. Instead, two basins (above and below the C position) appeared, but they were not oriented toward the pnicogen. This was also noted in the appearance of a lobe (not a basin) below the C atom, which was fused with both valence C−Si basins, causing these basins to have a population >2 for containing half of the lower lobe. For **1d**−**6d** compounds, with the F and SiH_3 groups, the effects were similar to those mentioned above, but for the organic ylides **4d**−**6d** the double bond was reinforced due to the convergence of both effects in the disruption of the lone pair at the carbon atom (see Supporting Information, Figures S2 and S3).

This leads us to propose a general bonding scheme for these ylides and their boron analogues. The N−Y bond in the unsubstituted compounds is a dative single one which, after F substitution, turned into a double one. The restrictions (in its valence) for the N atom to form five bonds forces the breakdown of one of the F−N covalent bonds, augmenting the F−N distance and changing it into an ionic one, thus forming the above-mentioned complexes. For the remaining pnicogen (P, As) ylides, the situation was different. For the organic ylides, the unsubstituted molecules showed a clear but relatively weak double X−C bond that is progressively strengthened after F and SiH_3 substitutions at the X and Y atoms, respectively. There was a charge redistribution from the carbon lone pair to the central bond that became double, these changes being induced mainly by the F substituents. However, the boron compounds showed remarkably different bonds. The ELF basins for the lone pairs of phosphine and arsine moieties were not located directly toward the B atom, but rather sideways. Accordingly, the electron-pairing basin in the bond region was divided into two basins, each belonging to X and B atoms.

IV. Rotational Barriers. We also explored the rotational barriers for further analysis of the X−Y bonding nature. Considering the scant differences induced by the SiH_3 groups and the approximated behavior of P and As compounds, we performed the potential energy scan only for **1**, **2**, **4**, and **5** (**a**,**b**).

This scanning had to be executed carefully, due to the special geometric and bonding characteristics for these ylides, in order to achieve accurate determinations of the magnitudes we intend to explore. In our case, we tested the multiplicity of the central

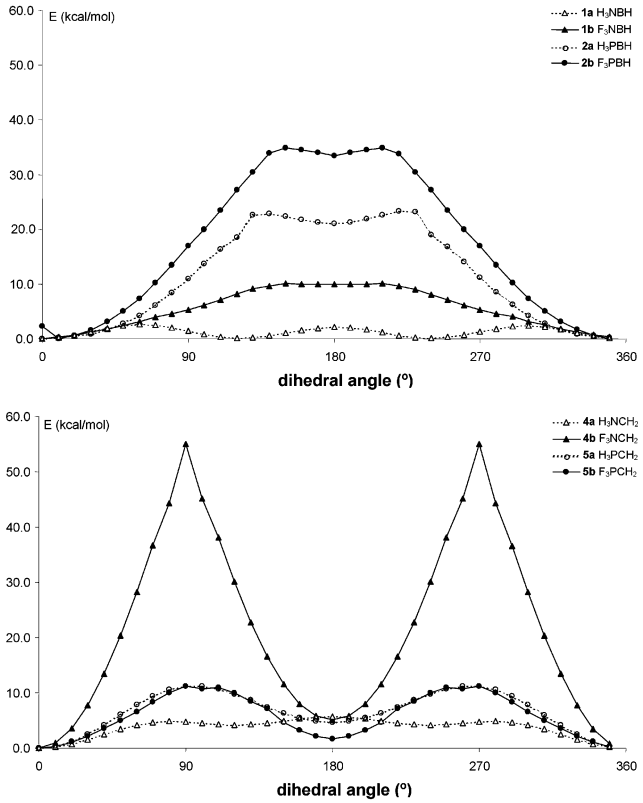

Figure 3. Restricted potential-energy curves corresponding to the torsion around X−B (top) and X−C (bottom) bonds for **1**,**2**(**a**,**b**) and **4**,**5**(**a**,**b**), respectively, at the CAS(2,2)MP2/6-311+G*//MP2/6-311+G* level.

bond, and therefore, in order to estimate the double-bond strength, the torsion has to break the double bond at ca. 90°. For comparing the rotational barrier with the experimental values, the most correct procedure involves a relaxed scanning. However, due to the geometric aspects for these molecules, a relaxed scan leads to the initial conformation every 120°, after the optimization, yielding lower values for the barriers (ca. 1 kcal/mol) and a periodic potential energy curve. Therefore, a hypothetical double bond could not be broken during the dihedral angle torsion in a relaxed scan because the same conformation would appear at 0°, 120°, and 240°.

The calculated potential energy scans are depicted in Figure 3. Filled symbols correspond to the fluorinated molecules. The curves for **1a** and **4a** were below 5 kcal/mol and showed three alternative maxima and minima, corresponding to a clear single-bond rotation where the 3-fold symmetry results from repulsion between substituents. On the contrary, upon fluorination, these compounds showed remarkable rotational barriers (ca. 55 and 10 kcal/mol for organic ylides and their boron analogues, respectively). However, the remaining phosphonium ylides showed pronounced patterns regardless of the substituents. All the above trends supported the bonding-nature scheme discussed above. The barrier heights for the F derivatives were generally more pronounced than those from the unsubstituted molecules, indicating that the double-bond character was reinforced.

In addition, for the remaining curves, there was also a substantial difference in the positions of the maxima between the boron and carbon compounds. The organic ylides (Figure 3, bottom) showed two maxima located at 90° and 270° and two similar minima at 0° and 180°, while the boron analogues (Figure 3, top) showed the maxima at values >100° and a relative minimum at 180°, raised to values near those of the maxima. This supports the bonding scheme proposed previously

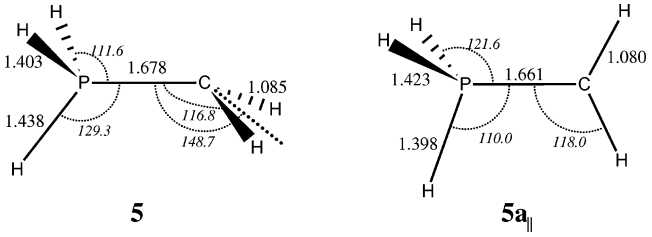

Figure 4. Geometric details for **5a** and its rotamer **5a**$_{||}$, at the MP2/6-311+G*//MP2/6-311+G* level.

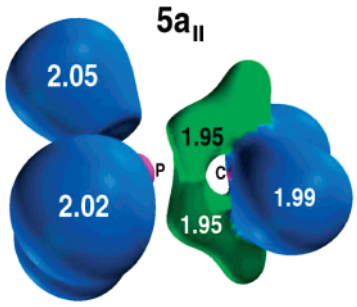

Figure 5. ELF representation at 0.7 for rotamer **5a**$_{||}$, at the B3LYP/6-311+G*//B3LYP/6-311+G* level.

for second-row and beyond X atoms. The reinforcement of the central P−C and P−B bonds ylides, visible in the rotation potential energy curve, is moderate, as happened similarly with the electronic properties. Even after fluorination, the same bond characteristics (double-bond barrier in **5a** and a barrier with a very high relative minimum in **2a**) were already present, yielding only to quantitative changes, not qualitative as observed in the ammonium compounds.

The P−B bond showed different characteristics, not presenting a neat single- or double-bond character. This is especially clear for compounds **2a** and **2b**, because at 180° the lone pairs of the phosphine moiety and the boron atom repelled each other. This repulsion resulted in values at 180° close to those of the maxima. For **1b**, whose central N−B bond had been considered as double, the maxima were nearer 90°, in accordance with its higher double-bond character, although the energy difference between the two minima persisted. The repulsion effects at 180° were not as clear as in **1b**, but the difference of ca. 12 kcal/mol accounted for the relatively high volume and population of the lone pair, in comparison with **4b** (see ELF representations in Figure 2). This remarks the importance of the rigid scan. In the case of a relaxed scan, the aforementioned differences would have been masked had the phosphine and ammonia units been allowed to rearrange in such a way that their lone pairs avoided each other.

On the graphs presented, the rotational barrier of ca. 10 kcal/mol in the phosphonium ylide **5a** clearly indicates the presence of a double bond, although the barrier is relatively low in comparison with a conventional P═C bond. This contrasts with numerous reports in the literature[10,11,36] concerning these values, where all the authors agree on a low rotational barrier <1 kcal/mol. The rotational barriers reported here preserved the rest of the geometry intact, while the values reported in the literature were obtained as the difference between two optimized conformations, the minimum **5a** and the rotamer with a planar CH_2 group turned 90° (called **5a**$_{||}$ in Figure 4).

To explain these differences, we calculated and analyzed the same structures used by Molina,[10] Eades,[36] and, more recently, Nyulászi.[11] The resulting optimized geometries are depicted in Figure 4, both showing C_s symmetry. The CH_2 group was kept planar, but both CH distances and PCH valence angles were able to optimize, as was the PH_3 moiety. The energy difference between the **5a** and **5a**$_{||}$ proved to be 1.3 kcal/mol, calculated at the MP2 level, and 1.2 kcal/mol at the B3LYP level, in agreement with the results reported.

The differences between these two approaches for evaluating the double-bond character of the P−C bond requires further explanation. For molecules such as ethylene, the energetic comparison between the different conformers with the CH_2 groups parallel and perpendicular is an appropriate technique for analyzing the double-bond strength, but here the situation is different. In ethylene, a 90° turn produces perpendicular orientation of the p_z orbitals, avoiding the formation of a double bond. Contrarily, in **5a**, due to the approximate local C_3 symmetry of the H_3P group, there is always a similar overlap between the carbon p_z orbital and those hybrid in X.

Nevertheless, there are mainly two geometric features that lead to a different orbital overlap in compounds similar to **5a**, depending on the relative orientation of both groups. The first feature consists of the different positions of the substituents attached to P, denoted by a heading angle $\gamma > 109°$, and the second is the nonplanarity of the CH_2 group. This is why the geometries of the substituents were preserved during the scan, in order to clarify how the electronic environment around the P atom affected the bond multiplicity in **5a**.

The discrepancies in the two procedures for the rotational barrier estimation can be explained more specifically from the geometric data displayed in Figure 4. There were noticeable changes in the PH_3 group after rotating by 90° a planar CH_2 group, consisting of the shortening of the P−C bond as well as the reduction of the P−H bond and valence angle located in the symmetry plane, while the remaining P−H bonds were lengthened and located away from the central bond. These effects cannot be attributed to the hydrogen repulsion, because in the **5a**$_{||}$ rotamer, with two H atoms eclipsed with themselves, the in-plane P−H bond was displaced toward the central P−C bond, with any kind of repulsion not existing.

Moreover, the double-bond strength calculated as the energetic difference between **5a** and **5a**$_{||}$ is demonstrated to be inapplicable here, after the electronic structures of both rotamers are compared. A detailed AIM and ELF analysis of the bond characteristics for **5a**$_{||}$ yielded the ELF plot depicted in Figure 5, where two pairing basins with high population (1.95 e) were located over and under the P−C bond, slightly extended toward the carbon. This, together with a shorter bond length in **5a**$_{||}$ and the forced sp^2 hybridization, indicated clearly that the bond in **5a**$_{||}$ had even more double-bond character than had **5a**. Therefore, the values reported in the literature do not estimate the double-bond strength; rather, they compare the relative stability of the different rotamers with similar double-bond character. The double bond is not broken in **5a**$_{||}$ and, therefore, does not constitute a reference for comparing the double-bond character in **5a**.

From all the above, structure **5a**$_{||}$ can be considered a transition state between two of the three configurations equivalent to **5a** which the molecule encounters during a 360° rotation. In **5a**$_{||}$, the double bond is preserved, but this does not mean that the π-bond cannot be broken. Rather, it cannot be broken in this way. For an estimation of the strength of a double bond, the dihedral angle has to be rotated, preserving the geometric conditions that allowed the bond to be double. These conditions consist of the same τ- and γ-angles for the carbon planarity and orientation of the PH_3 moiety, respectively, as well as the same bond distances with H. All of the above explains the differences between the rotational barriers reported in the

literature[10,11,36] and the values presented in the present work, removing a key argument for considering the central bond in **5a** as single.

Conclusions

The ylides and boron derivatives studied in this work presented different characteristics for the central X−Y bond. For conventional organic ylides, the behavior ranged between two extreme situations, one with X−C central single bond and a sp^3 carbon atom, and the other with a X−C double bond and a sp^2 carbon. The resemblance to one of those models depends strongly on the substituents at the central bond and the subsequent electronic displacement induced by them. For the double-bond character (ylene form) to be increased, the carbon lone pair has to be destroyed and its charge directed toward the bond. This is accomplished by the F substituents attached to X that pull charge from the bond, but not by the SiH_3 groups that push charge at the C atom, whose presence was noted only as a steric repulsion.

On the other hand, the boron analogues presented a different situation. Although there were similarly two extreme forms, where the X−B bonds appeared as single and double, the intermediate situations differed due to a clear bond asymmetry. From the ELF analysis, we concluded that the paired electrons participating in the bond were not located directly between the X and B atoms, but sideways. This anisotropy was also reflected in the rotational barriers with a maximum close to 180° and values ca. 30 kcal/mol, produced by repulsion between pairing basins from X and B.

Among all the pnicogen atoms, N showed the highest variability on substitution, presenting the most single- and double-bond characters in **1a**, **1b**, **4a**, and **4b**. Although all of these receive the same ylide denomination, our analysis indicated a clear bond difference between the ammonium and the other ylides.

Also, the present study has used different topological, energetic, and geometric analyses for the determination of the bond multiplicity. Several structural and electronic effects showed that some increases in the bond multiplicity are not reflected in the delocalization indices, indicating that future multiplicity estimations cannot be performed with only a single parameter, such as the electron-delocalization index. Our results for the potential-energy scan revealed barriers higher than 10 kcal/mol, indicating that the disputed nature of the P−C bond on the phosphonium ylide **5a** has to be considered as a double, especially in the presence of highly electronegative substituents. The barriers reported in the literature[10,11,36] (pointing out values <1 kcal/mol) should not be considered incorrect, because they are intended to reproduce the experimental rotation barrier but not the double-bond strength; therefore, these values should not be used as an argument against the double bond. Moreover, the conformation corresponding to the maximum in a relaxed scan (**5a**$_{||}$) also presented a double-bond character, and therefore the energy differences between the rotamers **5a** and **5a**$_{||}$ is not indicative of the double-bond strength.

Acknowledgment. This work was financed by Ministerio de Ciencia y Tecnología (BQU2002-01207). Computing time was provided by the Universidad de Granada. We are grateful to Professors R. F. W. Bader and B. Silvi for supplying us a copy of the AIMPAC and ToPMoD software packages. Mr. David Nesbitt corrected the original English manuscript.

Supporting Information Available: Laplacian representations for **4a** and **5a** (Figure S1) and ELF representations for **1c**−**6c** and **1d**−**6d** (Figures S2 and S3). This material is available free of charge via the Internet at http://pubs.acs.org.

References and Notes

(1) Clark, J. S. *Chemistry. A Practical Approach in Chemistry*; Oxford University Press: Oxford 2002.

(2) Stevens, T. S.; Creighton, E. M.; Gordon, A. B.; MacNicol, M. *J. Chem. Soc.* **1928**, 3193.

(3) Kolodiazhhnyi, O. I. *Phosphorus Ylides*: *Chemistry and Application in Organic Synthesis*; Wiley-VCH: New York, 1999.

(4) Maryanoff, B. E.; Reitz, A. B. *Chem. Rev.* **1989**, *89*, 863.

(5) Li, A. H.; Dai, L. X.; Aggarwal, V. K. *Chem. Rev.* **1997**, *97*, 2341.

(6) Dobado, J. A.; Martínez-García, H.; Molina, J.; Sundberg, M. R. *J. Am. Chem. Soc*. **2000**, *122*, 1144.

(7) Naito, T.; Nagase, S.; Yamataka, H. *J. Am. Chem. Soc*. **1994**, *116*, 10080.

(8) Dransfeld, A.; Forro, A.; Veszprémi, T.; Flock, M.; Nguyen, M. T. *J. Chem. Soc., Perkin Trans. 2* **2000**, 2475.

(9) Bachrac, S. M. *J. Org. Chem.* **1992**, *57*, 4367.

(10) Molina, P.; Alajarin, M.; Lopez, C.; Claramunt, R. M.; Foces, M. C.; Hernández, F.; Catalan, J.; de Paz, J. L.; Elguero, J. *J. Am. Chem. Soc.* **1989**, *111*, 355.

(11) Nyulászi, L.; Veszprémi, T.; Réffy, J. *J. Phys. Chem.* **1995**, *99*, 10142.

(12) Nyulászi, L.; Veszprémi, T. *J. Phys. Chem.* **1996**, *100*, 6456.

(13) Reed, A. L.; Weinhold, F. *J. Am. Chem. Soc.* **1986**, *108*, 3586.

(14) Reed, A. L.; Schleyer P. v. R. *J. Am. Chem. Soc.* **1990**, *112*, 1434.

(15) Magnusson, E. *J. Am. Chem. Soc*. **1990**, *112*, 7940.

(16) Gilheany, D. G. *Chem. Rev.* **1994**, *94*, 1339.

(17) Chesnut, D. B. *Heteroat. Chem.* **2000**, *11*, 341.

(18) Mitrasinovic, P. M. *J. Comput. Chem.* **2001**, *22*, 1387.

(19) Mitrasinovic, P. M. *J. Phys. Chem. A* **2002**, *106*, 7026.

(20) Mitrasinovic, P. M. *Chem. Phys.* **2003**, *286*, 1.

(21) Møller, C.; Plesset, M. S. *Phys. Rev.* **1934**, *46*, 618.

(22) Becke, A. D. *J. Chem. Phys.* **1993**, *98*, 5648.

(23) Lee, C.; Yang, W.; Parr, R. G. *Phys. Rev. B* **1988**, *37*, 785.

(24) Frisch, M. J.; Trucks, G. W.; Schlegel, H. B.; Scuseria, G. E.; Robb, M. A.; Cheeseman, J. R.; Zakrzewski, V. G.; Montgomery, J. A., Jr.; Stratmann, R. E.; Burant, J. C.; Dapprich, S.; Millam, J. M.; Daniels, A. D.; Kudin, K. N.; Strain, M. C.; Farkas, O.; Tomasi, J.; Barone, V.; Cossi, M.; Cammi, R.; Mennucci, B.; Pomelli, C.; Adamo, C.; Clifford, S.; Ochterski, J.; Petersson, G. A.; Ayala, P. Y.; Cui, Q.; Morokuma, K.; Rega, N.; Salvador, P.; Dannenberg, J. J.; Malick, D. K.; Rabuck, A. D.; Raghavachari, K.; Foresman, J. B.; Cioslowski, J.; Ortiz, J. V.; Baboul, A. G.; Stefanov, B. B.; Liu, G.; Liashenko, A.; Piskorz, P.; Komaromi, I.; Gomperts, R.; Martin, R. L.; Fox, D. J.; Keith, T.; Al-Laham, M. A.; Peng, C. Y.; Nanayakkara, A.; Challacombe, M.; Gill, P. M. W.; Johnson, B.; Chen, W.; Wong, W.; Andres, J. L.; Gonzalez, C.; Head-Gordon, M.; Replogle, E. S.; Pople, J. A. *Gaussian 98*, Revision A.11.4; Gaussian, Inc.; Pittsburgh, PA, 2002.

(25) Bader, R. F. W. *Atoms in Molecules: A Quantum Theory*; Clarendon Press: Oxford, 1990.

(26) Bader, R. F. W. *Chem. Rev.* **1991**, *91*, 893.

(27) Becke, A. D.; Edgecombe, K. E. *J. Chem. Phys.* **1999**, *98*, 5397.

(28) Biegler-Köning, F. W.; Bader R. F. W.; Tang, T. H. *J. Comput. Chem.* **1982**, *3*, 317.

(29) Noury, S.; Kokridis, X.; Fuster, F.; Silvi, B. *ToPMoD*; Laboratoire de Chimie Théorique, Université Pierre et Marie Curie: Paris, 1999.

(30) Pepcke, E.; Lyons, J. *SciAn 1.2*; SCRI, Florida State University: Tallahassee, 1996.

(31) Synaptic order is defined for a valence basin as the number of connections with core basins. Hydrogenated basins, although they do not contain core basins, are considered disynaptic if they contain H nuclei.

(32) The different substitutions are marked with **a**−**d**, indicating **a** the unsubstituted molecules, **b** those with F bonded to X, **c** those with the SiH_3 group bonded to Y, and finally **d** presenting both substitutions.

(33) Defined as the ratio between the most pronounced curvatures in the electron density minus one, $\epsilon = 1 - \lambda_1/\lambda_2$, computed at the BCP.

(34) Chesnut, D. B. *J. Phys. Chem. A* **2003**, *107*, 4307.

(35) Chesnut, D. B. *Chem. Phys.* **2001**, *271*, 9.

(36) Eades, R. A.; Gassman, P. G.; Dixon, D. A. *J. Am. Chem. Soc.* **1981**, *103*, 1066.